Novel compatibilizers and plasticizers developed from epoxidized and maleinized chia oil in composites based on PLA and chia seed flour

Ivan Dominguez-Candela [a],[*], Jaume Gomez-Caturla [b], S.C. Cardona [a], Jaime Lora-García [a], Vicent Fombuena [b]

[a] *Instituto de Seguridad Industrial, Radiofísica y Medioambiental (ISIRYM) Universitat Politècnica de València (UPV), Plaza Ferrándiz y Carbonell, s/n 03801, Alcoy, Spain*
[b] *Technological Institute of Materials (ITM), Universitat Politècnica de València (UPV), Plaza Ferrándiz y Carbonell 1, 03801 Alcoy, Spain*

ARTICLE INFO

ABSTRACT

Novel compatibilizers and plasticizers derived from epoxidized chia seed oil (ECO) and maleinized chia seed oil (MCO) have been applied in composites based on poly(lactic acid) (PLA) and 15 wt% chia seed flour (CSF). Results obtained have been compared to conventional silane coupling agent, (3-glycidyloxypropyl) trimethoxysilane (GPS), and a petroleum-based compatibilizer, poly(styrene-co-glycidyl methacrylate) copolymer (Xibond, ®). The compatibilization effect of green composites were assessed by FTIR. The addition of all four compatibilizers improved the ductile mechanical and thermal properties of the composites. The morphology analysis revealed an improvement of interfacial adhesion of the CSF particles into the PLA matrix. In particular, ECO and MCO composites showed a roughness with long filaments in their morphology which plays a crucial role in improving the ductile properties highly. The elongation at break was 10 and 8 times higher using ECO and MCO, respectively, compared to uncompatibilized composite. Moreover, the composites manufactured showed low values (<9%) in the water uptake assay and a negligible compostability delay. The use of novel compatibilizers based on modified vegetable oils could mean an interesting proposal to obtain an entirely environmentally friendly composite with a remarkable ductile property.

1. Introduction

At present, one of the leading environmental concerns is the continuous generation of plastic wastes after human consumption. In Europe, plastics production reached 62 million tonnes in 2018, of which 29 million tonnes were collected to be treated [1]. Despite this target, 7.25 million tonnes were still sent to landfills. Therefore, an interesting proposal to overcome this environmental problem is to substitute the most commonly used petrochemical and non-biodegradable plastics, known as *commodities* (LDPE, HDPE, PVC, PP, PS, etc.), by bioplastics, i. e., polymers that are biodegradable, bio-based or both features.

Regarding bioplastics, the most remarkable are the biodegradable and fully or partially bio-based polymers, because they allow reducing the dependency of fossil resources and, therefore, greenhouse gas emissions. Poly(lactic acid) – (PLA) is one of the most used biodegradable polymers due to its competitive price, the suitable thermal stability to be industrially processed, good mechanical properties that can be compared to several non-biodegradable polymers, high transparency,

etc. [2]. For these reasons, PLA involves 24% of the global market production of biodegradable polymers, followed by poly(butylene succinate) (PBS) and poly(butylene adipate-co-terephthalate) (PBAT) with a value of 23% [3]. Nevertheless, the major drawback is its inherent brittleness and poor compatibility with organic fillers, as those that can be used to develop green composites, making some commercial applications difficult.

Thus, improving the ductile properties and enhancing the interfacial adhesion between organic fillers and polymeric matrix are two of the most critical challenges for the biopolymers and composites PLA-based sector. In previous literature, several strategies have been performed based on the physical and chemical processes of lignocellulosic filler. Some physical methods based on plasma treatment and ultraviolet radiation with interesting results were obtained using lignocellulosic filler [4,5]. Besides, conventional chemical surface treatments on fillers such as acetylation [6], esterification [7], or alkaline procedure [8] were also studied. In addition, one of the most used chemical surface treatments is silanization, which employs a silane coupling agent to improve the

matrix-particle interaction. Numerous reports have demonstrated the effectiveness of treating the lignocellulosic filler with a silane coupling agent [9–11]. However, currently, the straightforward strategy is regarding the use of reactive compatibilizers. In this case, the compatibilizers used are based on polymers with reactive groups that form new chemical bonds between matrix and lignocellulosic particles during melt processing [12]. Recent researches are focusing on the functionalization of vegetable oils due to their several reactive groups present in their chemical structure. So far, the most employed and available commercially vegetable oils are based on epoxidized and maleinized linseed and soybean oils [13–16]. However, there is practically no literature on the use of chia seed oil (CO) from *Salvia hispanica. L.*, one of the vegetable oils with the greatest potential due to its high unsaturated fatty acid content.

CO is a promising vegetable oil due to the high availability of double bonds, even higher than linseed oil, making it suitable to be chemically modified by diverse reactions. In a previous study, CO was subjected to an epoxidation process to obtain a bio-based plasticizer to be applied in the PLA matrix, giving rise to a successful behaviour [17]. On the other hand, the maleinization process of the CO has never been reported in previous literature, as far as we know. For this reason, the main objective of the present work is to compare the employment of epoxidized chia seed oil (ECO) and maleinized chia seed oil (MCO) with a conventional silane coupling agent, i.e., (3-glycidyloxypropyl) trimethoxysilane (GPS), and a petroleum-based compatibilizer, i.e., poly(styrene-co-glycidyl methacrylate) random copolymer (Xibond), as plasticizers and compatibilizers in composites based on PLA and organic fillers.

As organic filler, the lignocellulosic waste from chia seed after oil extraction has been employed in flour form. This organic filler, which is chia seed flour (CSF), should be taken into account because the annual growth rate of CO from 2019 to 2025 is expected to be around 23% [18]. Moreover, considering the high CO production trend corresponding to 20% of the market share of chia seed and that the lignocellulosic waste is approximately 70% of whole chia seeds, a large amount of wastes is being generated. In order to contribute to circular economy and add value to this high amount of by-product in CO production, CSF is considered an interesting candidate to be employed in polymer industry to obtain high environmentally friendly composites. The addition of this filler was also reported previously in bio-based high-density polyethylene, becoming a composite partially biodegraded [19].

Therefore, to develop a more circular economy model in polymeric products applicable to sectors such as packaging, automotive, or even interior design, a novel fully biodegradable composite has been developed using PLA and lignocellulosic wastes from CO production. Mechanical, thermal, morphological, water uptake, and disintegration by composting tests have been used for comparing plasticizers and compatibilizers based on epoxidized and maleinized chia oil with coupling agents based on silanes and poly(styrene-co-glycidyl methacrylate) for the first time.

2. Experimental

2.1. Materials

The aliphatic polyester PLA used in this work was a commercial-grade 6201D supplied in pellet form by NatureWorks LLC (Minnetonka, Minnesota, USA). This PLA has a density of 1.24 g·cm^{-3} and an approximate molecular weight of 120,000 g·mol^{-1}. The melt flow index (MFI) is 15–30 g·(10 min)$^{-1}$ measured at 210 °C and using a nominal load of 2.16 kg, which is suitable for injection molding.

Edible chia seed (*Salvia hispanica, L.*) was supplied by Frutoseco (Bigastro, Alicante, Spain). CO was obtained from edible chia seed by a cold mechanical extraction method using a CRZ-309 press machine (Changyouxin Trading Co., Zhucheng, China). The residual cake obtained was subjected to mill process using an ultra-centrifugal mill from Retsch GmbH (Düsseldorf, Germany) working at a rotating speed of

8000 rpm with 0.25 mm sieve. As a result of this process, chia seed flour (CSF) was obtained as a lignocellulosic filler.

Concerning compatibilizers, a silane coupling agent (3-glycidyloxypropyl) trimethoxysilane (GPS) was obtained from Sigma Aldrich (Madrid, Spain). The GPS density is 1.07 g·cm^{-3} with a molecular weight of 236.34 g·mol^{-1}. As a petrochemical compatibilizer, Xibond^{TM} 920 was used, which is a poly(styrene-co-glycidyl methacrylate) random copolymer supplied by Polyscope (Geleem, The Netherlands). It presents a molecular weight value of 50,000 g·mol^{-1}, a glass transition temperature of 95 °C, and a glycidyl methacrylate content of 20% mole fraction. Finally, as a bio-based compatibilizer, CO was employed with two different chemical modifications: epoxidation and maleinization. The epoxidation process of CO was carried out as indicated in a previous report [17]. ECO presents an epoxy content of 6.71% with an iodine value of 25 g I$_2$·(100 g)$^{-1}$ and density of 1.026 g·cm^{-3}, following the guidelines of ASTM D1652, ISO 3961, and ISO 1675, respectively. The maleinization process was performed by adding maleic anhydride (MA) with purity > 98% supplied by Sigma Aldrich (Madrid, Spain). A total of 9 g of MA per 100 g of CO was used following the method reported by Lerma-Canto *et al.* [20]. MCO presents an acid value of 120 mg KOH·g^{-1} according to ISO 660, a density of 1.040 g·cm^{-3}, and an iodine value of 104 g I$_2$·(100 g)$^{-1}$. The chemical structure of each compatibilizer is shown in Fig. 1.

### 2.2. Preparation of PLA/CSF composites with compatibilizers

Previously to the preparation of composites, PLA, CSF, and Xibond were dried at 40 °C over 36 h using an air oven to remove the residual moisture. All samples were weighed according to the proportions gathered in Table 1 and following the recommendations of the previous related literature. All mixed compositions were processed in a twin-screw co-rotating extruder from Dupra S.L. (Castalla, Alicante, Spain) at a constant rate of 40 rpm. The temperature profile was set from the hopper to the die as follows: 162.5 °C, 165 °C, 170 °C, and 175 °C. After this, samples obtained were air-cooled at room temperature and pelletized. Before injection, all samples were dried again at 60 °C for 24 h. Afterwards, each formulation was shaped into pieces by injected molding from Mateu & Solé (Barcelona, Spain) and PLA/CSF composites with different compatibilizers were obtained. The temperature profile was set as follows: 190 °C (hopper), 195 °C, 197 °C, and 200 °C (injection nozzle). Regarding cavity filling and cooling time, they were set to 1 s and 10 s, respectively.

2.3. Infrared spectroscopy

Fourier-transformed infrared spectroscopy (FTIR) was performed using a Bruker S.A. Vector 22 (Madrid, Spain). FTIR instrument was coupled to single reflection attenuated total reflectance (ATR) accessory with a diamond ATR crystal (Madison, Wisconsin, USA). Each scan was collected using a wavelength between 400 and 4000 cm^{-1} from 12 scans at 4 cm^{-1} of spectral resolution. All spectra were normalized using the Perkin-Elmer software Spectrum.

2.4. Mechanical characterization

Mechanical assays such as tensile, impact, and hardness tests were carried out to evaluate the influence of the compatibilization effect in PLA/CSF composites. The tensile characterization was carried out in a universal test machine Ibertest ELIB 30 from S.A.E. Ibertest (Madrid, Spain), using a 5 kN load cell and a crosshead rate of 10 mm·min^{-1}. Samples of size 150 × 10 × 4 mm^3 were used following the recommendation of the ISO 527. In addition, the tensile modulus was obtained accurately using an axial extensometer from S.A.E. Ibertest (Madrid, Spain). The impact strength was measured in a 1 J Charpy's pendulum from Metrotec S.A. (Madrid, Spain) with a sample size of 80 × 10 × 4 mm^3 according to the guidelines of the ISO 179. Regarding hardness, a

a) silane coupling agent
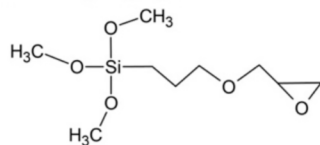
(3-glycidyloxypropyl) trimethoxysilane (**GPS**)

b) petroleum derived
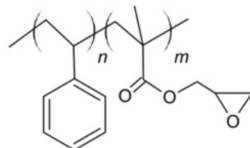
poly(styrene-co-glycidyl methacrylate)
random copolymer (**Xibond**)

c) vegetable oil derived (bio-based)
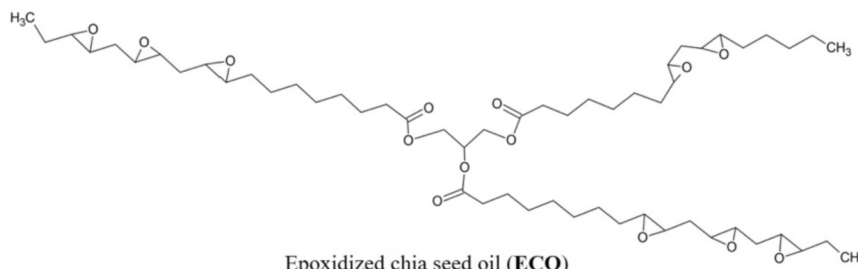
Epoxidized chia seed oil (**ECO**)
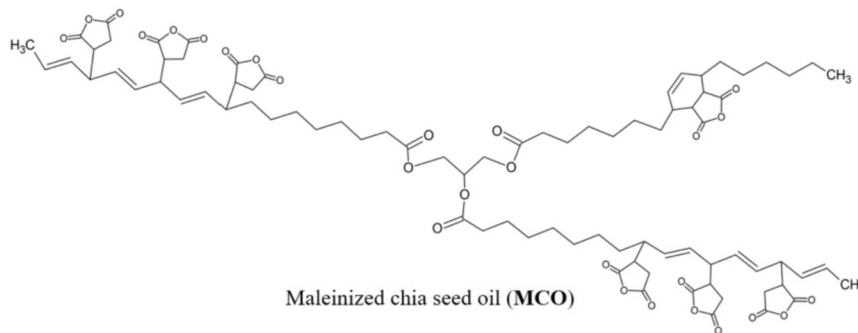
Maleinized chia seed oil (**MCO**)

Fig. 1. Scheme of the chemical structure of different compatibilizers used.

Table 1
Summary of compositions and codes of samples manufactured.

N° sample	PLA content (wt. %)	CSF content (wt. %)	Compatibilizer Employed	Compatibilizer content (wt. %)	Reference	Code
1	100	–	–	–		PLA
2	85	15	–	–	[21]	PLA/CSF
3	85	15	GPS	1[1]	[22–24]	PLA/CSF_S
4	84	15	Xibond	1[2]	[25]	PLA/CSF_X
5	77.5	15	ECO	7.5[2]	[17]	PLA/CSF_ECO
6	77.5	15	MCO	7.5[2]	[20]	PLA/CSF_MCO

[1] Respect to filler; [2] Respect to composite.

Shore D durometer model 676-D from J. Bot S.A. (Barcelona, Spain) was used as suggested by the ISO 868 standard. All mechanical tests were carried out at room temperature and at least five different specimens per sample were tested to obtain the average and deviation values.

2.5. Morphology characterization

The morphologies of fractured surfaces from the impact test of PLA/CSF with different compatibilizers were observed by field emission scanning electron microscopy (FESEM). This measurement was carried out in a ZEISS ULTRA 55 from Oxford Instruments (Oxfordshire, UK) using an acceleration voltage of 2 kV. Previously to observation, all fractured surfaces were coated with an Au-Pd alloy thin layer over 120 s under vacuum in a sputter coater EM MED020 from Leica Microsystems (Wetzlar, Germany). CSF sizes were measured by means of Image J Launcher v 1.52 k and the data presented was an average from 50 SEM micrographs.

2.6. Thermal characterization

The thermal behaviour of PLA/CSF with different compatibilizers was analysed by differential scanning calorimetry (DSC) and thermogravimetric analysis (TGA). The main thermal transitions of PLA/CSF composites were obtained by DSC in a Mettler-Toledo calorimeter 821e from Mettler Toledo Inc. (Schwerzenbach, Switzerland). The dynamic temperature program was set as follows: an initial heating from 30 °C to

300 °C to remove the thermal history, a cooling cycle from 300 °C to 30 °C, and finally a heating program from 30 °C to 300 °C. All samples with an average of 5–10 mg were subjected to a cooling and heating rate of 10 °C·min^{-1} according to ASTM D3418. All thermal cycles were carried out in nitrogen atmosphere with a constant flow rate of 66 mL·min^{-1}. The degree of crystallinity (X_c) of composites was determined using Eq. (1):

$$X_c \ (\%) = 100 \times \frac{\Delta H_m - \Delta H_{cc}}{\Delta H^0_{m(100\%)} \cdot w_{PLA}} \tag{1}$$

where ΔH_m and ΔH_{cc} stand for the melt and cold crystallization enthalpies (J.g^{-1}), respectively, w_{PLA} is the PLA weight proportion and $\Delta H^0_{m(100\%)}$ corresponds to the melt enthalpy of a theoretical fully crystalline PLA structure which is 93 J·g^{-1} [26].

The thermal stability of composites was evaluated by TGA analysis in a TGA/SDTA 851 thermobalance from Mettler-Toledo Inc. (Schwerzenbach, Switzerland). Samples with an average weight of 10 mg were subjected to a dynamic heating ramp from 30 to 700 °C at a constant heating rate of 10 °C·min^{-1}. All tests were carried out under a constant nitrogen flow (66 mL·min^{-1}). In addition, the first derivative thermogravimetric curves (DTG) were also obtained to evaluate the maximum degradation temperature of PLA/CSF composites.

2.7. Thermomechanical characterization

The dynamic mechanical thermal analysis (DMTA) of PLA/CSF with

different compatibilizers was evaluated in an oscillatory rheometer AR-G2 (TA Instruments, New Castle, USA). The changes in storage modulus (G') and damping factor (tan δ) were recorded in a torsion-shear mode with rectangular samples of size $40 \times 10 \times 4$ mm^3. Samples were subjected to a thermal program from 25 °C to 140 °C at a heating rate of $2 °C \cdot min^{-1}$, a maximum shear deformation (γ) of 0.1%, and a frequency of 1 Hz.

2.8. Water uptake

Samples of size $80 \times 10 \times 4$ mm^3 were immersed in distilled water at 23 ± 1 °C to evaluate the water absorption of PLA/CSF with different compatibilizers. The water uptake was carried out following the guidelines of the ISO 62. Previously to start the test, all samples were dried using an air oven at 50 °C for 24 h to remove the residual moisture. Three different samples of each composition were immersed to calculate the average and deviations values. Every week samples were taken out, dried using a dry cloth to remove the surface moisture, weighed in an analytical balance, and then immersed again to follow the water uptake evolution. The weight changes were measured for a period of 12 weeks. The water absorption (*W*) was calculated by the weight gain regarding the dried sample weight using Eq. (2):

$$W\ (\%) = 100 \cdot \frac{w_f - w_0}{w_0} \qquad (2)$$

where w_f is the final weight of the sample after taking it out each week and w_0 is the dry weight of the sample.

2.9. Disintegration under compost conditions

A disintegration test was carried out under anaerobic conditions at a temperature of 58 °C and relative humidity of 55%, as indicated by the ISO 20200. Seven different samples of each composition were shaped ($25 \times 25 \times 1$ mm^3) corresponding to each control day: 4, 8, 11, 15, 18, 23, and 31. Samples of each composition were dried in an air oven at 40 °C for 24 h. The dried samples were placed in a carrier bag and buried in a synthetic compost reactor ($300 \times 200 \times 100$ mm^3). At previously selected days, samples of each composition were unburied, washed, dried over 24 h, and subsequently weighed in an analytical balance while the remaining samples remained in the compost reactor. All tests were carried out in triplicate to ensure the reliability of the process. The percentage of weight loss (*W_L*) was determined by Eq. (3):

$$W_L\ (\%) = 100 \cdot \frac{w_0 - w}{w_0} \qquad (3)$$

where *w* is the final weight of the unburied samples for each control day after washing and drying and w_0 is the initial dry weight of the sample.

3. Results and discussion

3.1. FTIR analysis

To investigate the interaction of green composites, FTIR spectra of neat PLA and PLA/CSF composites were obtained as is shown in Fig. 2. Neat PLA presented two weak peaks attributed to antisymmetric and symmetric stretching vibration (–CH$_2$) at 2996 and 2962 cm^{-1}, respectively [27]. The three bands between 1500 and 1300 cm^{-1} are assigned to symmetric and antisymmetric deformational vibrations (C-H) in the methyl groups (CH$_3$) [28]. The strong peak located at 1748 cm^{-1} is ascribed to C = O stretching vibration of the carbonyl group [29]. Others strong peaks are observed between 1250 and 1000 cm^{-1} which are assigned to C-O and C-O-C stretching vibrations [30]. The addition of CSF in PLA matrix showed the same main peaks compared to PLA neat, although different intensity and/or shifts were observed, remarking at 1748, 1184 and 1078 cm^{-1}. This effect was also reported by Lima *et al.*
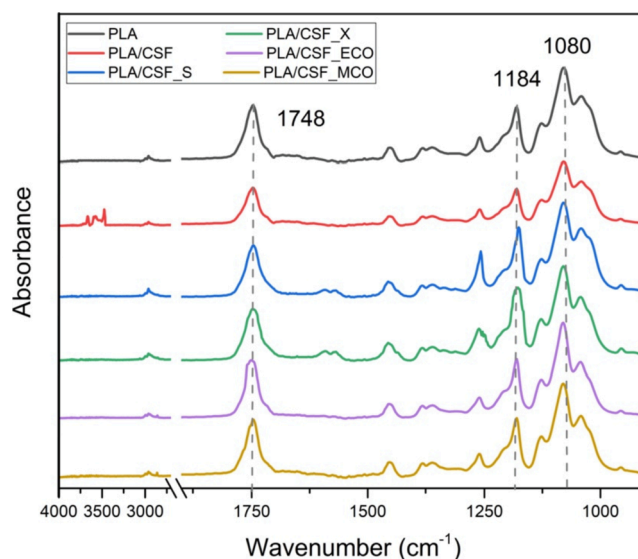

Fig. 2. FTIR spectra of poly(lactic acid) (PLA) and 15 wt% chia seed flour (CSF) composites with different compatibilizers.

[31] when the effect of 10–20 wt% of mango's kernel in PLA matrix was studied. These changes suggest that CSF addition interferes physically with PLA molecules hindering the movement [32]. Moreover, the new peaks are related to lignocellulosic filler, which might be not interacting completely with PLA. This peaks at 3500–3700 cm^{-1} are assigned to hydroxyl groups (–OH) stretching vibration present in the lignocellulosic filler of CSF [33].

Regarding the use of compatibilizers, the effect was observed compared to uncompatibilized PLA/CSF composite. In case of PLA/CSF_S composite, GPS coupling agent has two functional group: the first functional group is an alkoxy group that can be hydrolyzed to form active silanols, thus interacting with hydroxyl groups of lignocellulosic filler [34]; the second is an epoxy group that can link with hydroxyl end groups of PLA matrix leading the silane coupling agent to act as a chemical bridge [35]. In this regard, according to Garcia-Garcia *et al.* [36], this chemical interaction is associated to the contribution of bonds Si-O-Si and Si-O-C, which emphasize the peaks presents at 1108 cm^{-1} and 1220 cm^{-1}, respectively. This increase of intensity can be observed in PLA/CSF_S composite compared to uncompatibilized PLA/CSF composite, suggesting that new chemical bonds have been formed, which improve the interaction between filler and matrix. The addition of Xibond as compatibilizer showed an increase of intensity and shift at 1746, 1178 and 1078 cm^{-1}, suggesting interaction between CSF, PLA and compatibilizer. The glycidyl methacrylate functional group is highly reactive with condensation polymers such as PLA and lignocellulosic fillers by means of hydroxyl groups of both PLA and CSF filler [37]. In the case of functionalized vegetable oils in PLA/CSF composites, the chemical groups such as oxirane and maleic anhydride present in ECO and MCO, respectively, can react with the terminal hydroxyl groups of lignocellulosic filler, whereas the remaining groups are also available to react with hydroxyl groups of PLA chains [38,39]. Both showed a broader and shifted peaks at 1748, 1180 and 1080 cm^{-1} which suggests the intermolecular interaction between PLA, filler and bio-based compatibilizers as was reported in literature [40,41]. The presence of both modified vegetable oils showed a small peak at 2854 cm^{-1} that is attributed to the stretching vibration of –CH$_2$-CH$_3$ for incorporation of aliphatic chains [42]. In general, FTIR results suggest chemical interaction using all compatibilized composites compared to uncompatibilized PLA/CSF composite. In addition, a reduction of intensity between 3500 and 3700 cm^{-1} associated to hydroxyl groups in CSF filler structure was observed. This fact could also support the reaction between PLA and CSF filler by means of compatibilizers [43].

3.2. Mechanical properties of PLA/CSF composites with compatibilizers

Tensile properties of PLA/CSF composites with different compatibilizers are shown in Fig. 3(a). The tensile strength of neat PLA presented a value of 42 MPa that decreased up to 15 Mpa with the addition of 15 wt% of untreated CSF, as plotted in Fig. 3(a). It is worthy to note that CFS particles present a hydrophilic nature as common lignocellulosic fillers and, on the other hand, the PLA matrix is a hydrophobic polyester [44]. This results in a low interaction between CSF filler and PLA matrix, leading to a stress concentrator effect and subsequently decreasing the tensile strength [45]. With the surface treatment of CSF particles with GPS, an improvement of 19.2% compared to PLA/CSF composite was observed, probably due to the new bonds formed between CSF and PLA matrix by means of silane molecule. The addition of petrochemical copolymer Xibond recorded the highest tensile strength (21 Mpa), i.e., an increase of 35.4% with respect to PLA/CSF composite. In the case of bio-based functionalized vegetable oils, i.e., ECO and MCO, both presented the lowest tensile strength with a decrease of 63% compared to uncompatibilized PLA/CSF composite. This remarkable decrease is directly related to the plasticizing effect provided by modified vegetable oils, which causes a reduction of the tensile strength [46].
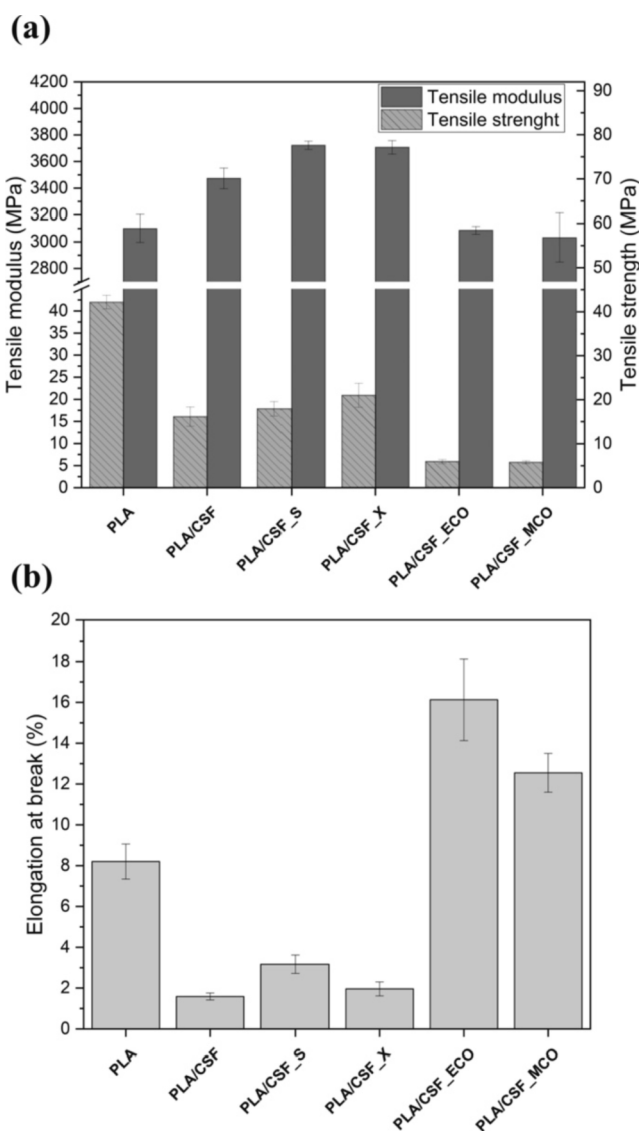
Regarding tensile modulus, the addition of 15 wt% of untreated CSF particles to the PLA matrix provided an increase from 3100 Mpa (neat PLA) up to 3500 Mpa. It is worthy to note that tensile modulus is related to the ratio of tensile strength to elongation at break, where both properties decrease because of the addition of CSF. In this case, the decrease of elongation at break was much more pronounced, leading to an increase in the tensile modulus, as observed in Fig. 3(a). The most remarkable values were obtained using PLA/CSF composites compatibilized with GPS and copolymer Xibond. Both presented similar values with an enhancement of 17.7 % compared to uncompatibilized PLA/CSF composite. This behaviour is typical of conventional compatibilizers that contribute to improving the stress transfer between matrix and particle, thus increasing the tensile modulus [12]. However, the addition of both modified vegetable oils led to obtaining the lowest values, 3050 Mpa approximately, which is a reduction of 15% compared to uncompatibilized PLA/CSF composite. This decrease agrees with values reported by Kamarudin *et al.* [47], who evaluated the addition of epoxidized Jatropha oil in PLA matrix with kenaf fiber as a filler. According to this study, the reduction of tensile modulus is related to the intrinsic flexibility that modified vegetable oils provide.

Concerning elongation at break, PLA is a hard but brittle polymer with a value of 8%, as shown in Fig. 3(b). As expected, the addition of 15 wt% of untreated CSF reduced the elongation at break up to 1.6% because of the loss of cohesion between filler and matrix. This property was slightly improved in PLA/CSF composites compatibilized with GPS and copolymer Xibond, enhancing the interfacial adhesion as mentioned above. In this case, CSF treated with GPS provided higher values than Xibond, obtaining a more ductile composite in both cases. Finally, the highest values were observed with the addition of functionalized vegetable oils in PLA/CSF composites. The elongation at break increased to 16% and 13% with ECO and MCO, respectively, which is 10 and 8 times higher than the PLA/CSF composite. It is known that some compatibilizers, particularly modified vegetable oils, act as plasticizers as well. On the one hand, the compatibilization effect with lignocellulosic filler has been reported. It is important to take into account that both oxirane and maleic anhydride present in ECO and MCO, respectively, can react with the terminal hydroxyl groups of lignocellulosic filler and PLA chains, leading to some potential reactions such as linear chain-extension, branching, and even cross linker structures, acting as a bridge [38,39]. On the other hand, they also present a plasticization effect that increases the free volume of PLA chains, thus increasing the chain mobility and consequently improving the ductile properties [48]. Therefore, modified vegetable oils can provide a dual function: a compatibilization effect due to an increase of polymer-filler interaction and plasticization effect. Similar behaviour was reported by Mahmud et al. [49] when evaluating the addition of epoxidized soybean oil (ESO) as a compatibilizer in PLA with cellulose powder.

Regarding impact-absorbed energy and Shore D hardness, results are summarized in Table 2. The brittleness of PLA was reflected in impact-absorbed energy with a value of 37.1 kJ/m^2. The incorporation of 15 wt% of untreated CSF induced a reduction up to 13.6 kJ/m^2, observing a decrease of 61% compared to neat PLA. This embrittlement of the composite is related to the weak interaction between CSF filler and PLA matrix, which causes a negative effect on the impact toughness. This result is in complete agreement with the tensile results obtained. For all

Fig. 3. Mechanical properties of poly(lactic acid) (PLA) and 15 wt% chia seed flour (CSF) composites with different compatibilizers; (a) tensile strength and modulus, (b) elongation at break.

Table 2

Impact-absorbed energy and Shore D hardness of poly(lactic acid) (PLA) and 15 wt% chia seed flour (CSF) composites with different compatibilizers.

Sample	Impact-absorbed energy (kJ/m^2)	Shore D hardness
PLA	37.1 ± 1.8	74.0 ± 2.3
PLA/CSF	13.6 ± 0.4	76.8 ± 3.2
PLA/CSF_S	15.7 ± 0.3	79.0 ± 2.6
PLA/CSF_X	15.6 ± 0.2	79.1 ± 2.0
PLA/CSF_ECO	16.5 ± 0.3	77.1 ± 2.4
PLA/CSF_MCO	16.2 ± 0.3	77.9 ± 1.6

tested PLA/CSF composites with compatibilizers, the toughness was improved, obtaining higher values than uncompatibilized PLA/CSF composite. The impact-absorbed energy is directly related to the chemical structure of compatibilizers and their ability to react with different components. In all compatibilization attained, the functional groups react with PLA and cellulose present in the CSF. As per results, both GPS and Xibond seem to give a similar enhancement of the toughness, being an improvement of 15.5% compared to uncompatibilized PLA/CSF. On the one hand, GPS compatibilizer presents a silanol group in one end that can react with hydroxyl groups of CSF, whereas the other functional group is an epoxy group that is linked to hydroxyl groups of PLA. On the other hand, Xibond compatibilizer, which contains a functional glycidyl methacrylate (GMA) group, is ready to react with both hydroxyl groups of CSF and PLA matrix, acting as a chemical bridge during the reactive extrusion process. The trend of impact-absorbed energy for the composites modified with vegetable oils was identical to the elongation at break, corroborating that polymer-matrix interaction has been improved and did not show significant differences. Therefore, the use of bio-based functionalized vegetable oils showed the highest impact-absorbed energy, as expected. The functional groups present in ECO and MCO, i.e., epoxy and maleic anhydride, respectively, can react with both hydroxyl groups contained in CSF and PLA matrix. As a result of this interaction, i.e., a compatibilization and plasticizing effect, the impact-absorbed energy has been improved. According to the previous elongation at break results, PLA/CSF_ECO composite also presented the highest toughness, suggesting higher reactivity than the MCO compatibilizer.

About Shore D hardness, neat PLA presented a value of 74.0 that increased up to 76.8 with the addition of 15 wt% untreated CSF, which is related to the intrinsic hardness of CSF. The addition of compatibilizers slightly improved the hardness compared to uncompatibilized PLA/CSF composite but, nevertheless, did not show significant differences considering the standard deviation. Similar behaviour was reported by Liminana *et al.* [50], who applied different compatibilizers in poly (butylene succinate) (PBS) composites with almond shell flour. However, considering the average value, the hardness achieved by modified vegetable oils was slightly lower than that of other compatibilizers due to the plasticization effect that ECO and MCO can provide.

3.3. Morphology of CSF and PLA/CSF composites with compatibilizers

The morphology of CSF particles observed by SEM at 500x as well as particle size distribution are shown in Fig. 4. As can be observed in Fig. 4 (a), the shape of CSF had an irregular morphology with tendency to form aggregates because of their elevated hydrophilicity. This morphology was also observed by Lascano *et al.* [51] who studied the shape of flax flour particles as filler in bio-based epoxy resin. Moreover, CSF particles showed rough surfaces that can be ascribed to the crushing process due to high hardness of this type of lignocellulosic filler. The distribution size of CSF particles, which was obtained with an average of 50 SEM images, was approximately 137μ m as shown in Fig. 4(b). The particle size plays an important role in the mechanical properties of green composites. Crespo *et al.* [52] reported that almond shell particle sizes higher than 150μ m could lead to mechanical impairment caused by greater heterogeneity of fillers within polymer matrix.

In the case of the surface morphology of fractured samples after Charpýs Impact test. Is gathered in Fig. 5. The first SEM image, Fig. 5(a), corresponds to a neat PLA sample which showed a smooth and flat surface typical of brittle polymers with no evidence of plastic deformation. In contrast, the addition of CSF particles, highlighted in yellow arrow in Fig. 5(b), increased the micro-crack formation. The lack of interaction between CSF particle and PLA matrix, highlighted in red arrow where an evident gap was observed, led to the loss of the continuity of composite. Consequently, CSF particles acted as a stress concentrator, which is in concordance with the previous brittle behaviour exposed in the mechanical test. In Fig. 5(c), the effect of silane treatment in CSF particles can be observed. In this case, CSF particles were better embedded in the PLA matrix with previous treatment with GPS, thus reducing the particle–matrix distance and obtaining an almost undetectable gap. The interfacial enhancement of particle–matrix interaction with silane coupling agent was also reported by several authors [53,54]. Similar morphology was observed with the addition of copolymer Xibond in PLA/CSF composite, indicating the enhancement of interaction as plotted in Fig. 5(d). This supports the above-reported mechanical results, where better compatibilization corresponds to an improvement of mechanical properties compared to untreated CSF/PLA composite. Regarding ECO and MCO compatibilizers, Fig. 5I and 5(f), both presented a good enough interaction due to the tiny gap between CSF and PLA matrix, as with previously commented compatibilizers occur. This fact could be ascribed to the compatibilization effect that
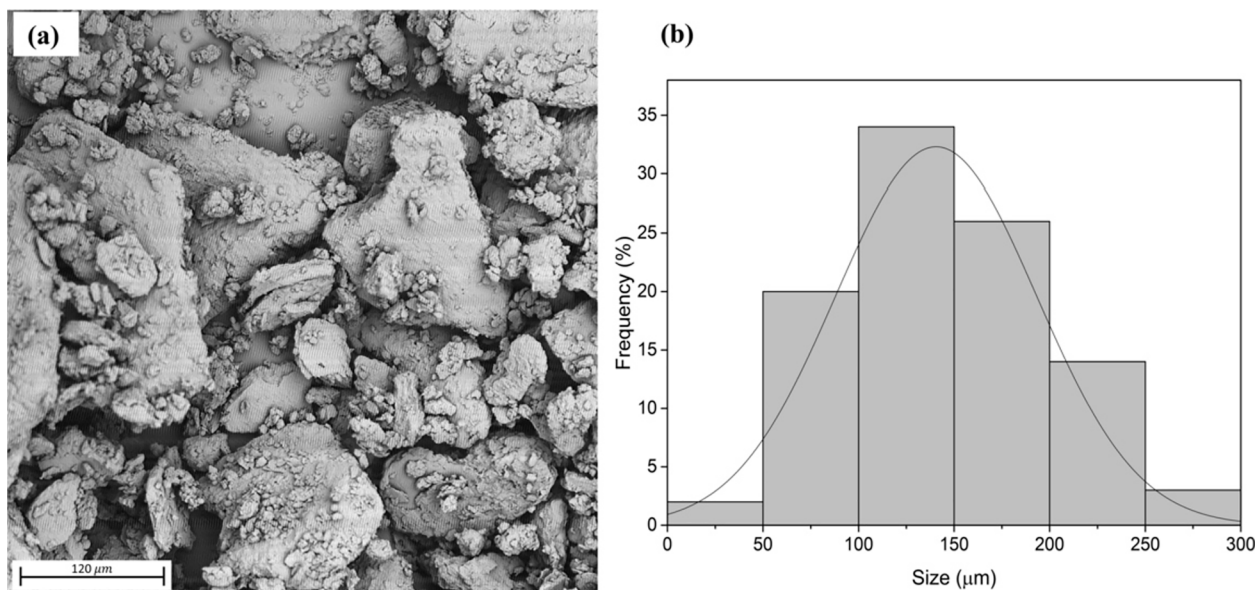

Fig. 4. (a) Surface morphology of chia seed flour (CSF) by field emission electron microscopy (FESEM) at 500x; (b) Histogram of CSF particles.
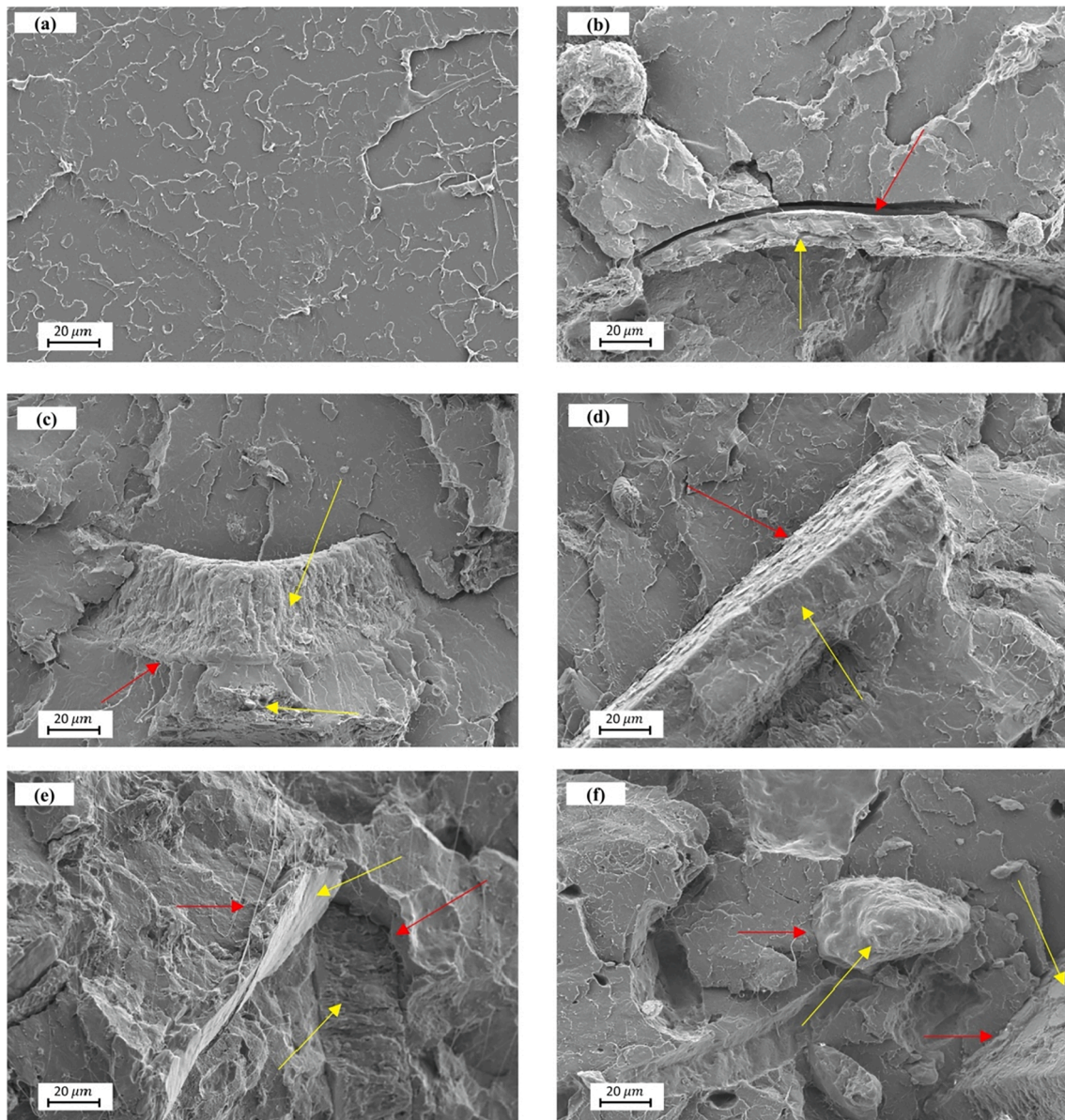
Fig. 5. Surface morphology of fractured samples by field emission electron microscopy (FESEM) of poly(lactic acid) (PLA) and 15 wt% chia seed flour (CSF) composites at 500x: (a) PLA; (b) PLA/CSF; (c) PLA/CSF_S; (d) PLA/CSI; (e) PLA/CSF_ECO; (f) PLA/CSF_MCO.

increase the interfacial adhesion due to chemical interaction. The reactive points of both modified vegetable oils, oxirane and anhydride maleic groups, can interact with hydroxyl groups of CSF and PLA matrix, leading to improvement of interfacial adhesion. Nevertheless, the matrix morphology showed a significant difference compared to PLA/CSF_S and PLA/CSF_X composites. The plasticization effect was observed due to the presence of characteristic long filaments from plastic deformation and a rougher surface [55] both in PLA/CSF_ECO and in PLA/CSF_MCO. Similar morphologies have been reported using different modified vegetable oils such as acrylated epoxidized soybean oil [56] or maleinized linseed oil [57] with fillers in PLA matrix. Comparing the morphology samples with the addition of ECO and MCO, no significant difference was observed, as shown in FigureI(e) and (f). Besides, it is known that modified vegetable oils are not completely miscible in the PLA matrix; thus, relatively high amounts can induce to form spherical voids that worsen the miscibility, with a negative effect on PLA ductile properties [13]. In a previous report [17], the ECO content was optimized in 7.5 wt%, obtaining a high improvement of ductile properties, i. e., 612% and 66% in elongation at break and impact-absorbed energy,

respectively. Although the gap between PLA and CSF was reduced and consequently a better mechanical interaction was obtained, the high results representative of a plasticizing effect (elongation at break and impact-absorbed energy) showed how the latter effect is more pronounced than the compatibilizer effect.

3.4. Thermal properties of PLA/CSF composites with compatibilizers

The thermal behaviour of neat PLA and PLA/CSF composites with different compatibilizers has been evaluated using DSC and TGA with a heating rate of 10 °C·min^{-1}. Table 3 gathered the main thermal parameters obtained from DSC. The first thermal transition, located at around 60 °C, corresponds to glass transition temperature (T_g). Firstly, neat PLA presented a T_g value of 62 °C that was reduced up to 60.4 °C with the addition of untreated CSF particles. This behaviour is related to the increment of free volume as well as chain mobility by loose packing of filler in the matrix due to a lack of interaction between them [58]. The same evolution was also reported by Ortiz-Barajas *et al.* [59] when introduced coffee husk flour in PLA. Regarding PLA/CSF_S and PLA/

Table 3

Main thermal properties of poly(lactic acid) (PLA) and 15 wt% chia seed flour (CSF) composites with different compatibilizers in terms of glass transition temperature (T_g), cold crystallization temperature (T_{cc}), cold crystallization enthalpy (ΔH_{cc}), melting Ierature (T_m), melting enthalpy (ΔH_m) and crystallinity (X_c).

Sample	T_g (°C)	T_{cc} (°C)	ΔH_{cc} (J·g⁻¹)	T_m (°C)	H_m Δ(J·g⁻¹)		X_c (%)
PLA	62.0 ± 0.7	119.4 ± 1.0	8.4 ± 0.7	150.2 ± 1.2	15.6 ± 1.3	7.7 ± 0.6	
PLA/CSF	60.4 ± 0.5	119.1 ± 1.2	24.3 ± 1.3	149.4 ± 0.8	25.2 ± 1.5	1.2 ± 0.3	
PLA/CSF_S	60.8 ± 0.9	115.9 ± 1.2	17.3 ± 0.5	148.6 ± 0.7	21.9 ± 0.7	5.8 ± 1.6	
PLA/CSF_X	61.3 ± 0.7	129.3 ± 1.3	1.10 ± 0.1	151.4 ± 1.3	2.3 ± 0.2	1.5 ± 0.2	
PLA/CSF_ECO	57.0 ± 1.0	129.5 ± 1.2	0.95 ± 0.1	151.2 ± 1.2	4.6 ± 0.5	5.1 ± 0.9	
PLA/CSF_MCO	59.6 ± 0.8	128.1 ± 1.1	2.16 ± 0.3	151.7 ± 1.3	7.5 ± 1.1	7.5 ± 0.9	

CSF_X composites, they presented a similar value in the 60.8–61.3 °C range, obtaining slightly higher values than PLA/CSF composite probably by the increase of the interfacial adhesion between CSF particles and PLA matrix [60]. Nevertheless, T_g values of functionalized vegetable oils presented an evident decrease of 59.6 °C and 57.0 °C for PLA/CSF_MCO and PLA/CSF_ECO composites, respectively. This effect supports the plasticizing effect that can be ascribed to the reduction of intermolecular forces, so inducing to increase its mobility [61]. Furthermore, these results are in concordance with the ductile properties where PLA/CSF_ECO composite presented the best ductility as well as the lowest T_g value, mainly due to the increase of the chain mobility. The second thermal transition is related to cold crystallization temperature (T_{cc}), being around 119.4 °C in the case of neat PLA. This value did not vary significantly with the addition of CSF particles. However, the lowest value was obtained for PLA/CSF_S composite, which is 115.9 °C, suggesting that previous silane treatment of CSF filler favours the crystal nucleation, thus shifting the T_{cc} at lower temperatures [62]. The use of Xibond, ECO, and MCO compatibilizers recorded a similar value in the 128.1–129.5 °C range, being almost 10 °C higher than PLA/CSF composite. This delayed of T_{cc} for the latter compatibilizers could be related to the formation of chain extended, branched, or even cross-linked structures of PLA with a higher impediment to crystallize [63]. In fact, this phenomenon also supports the low value of cold crystallization enthalpy recorded during heating scan as plotted in Fig. 6. The last thermal transition is related to the melting tempIure (T_m). Neat PLA showed a T_m value of 150.2 °C, whereas the addition of CSF particles only decreased about 0.8 °C. It is worthy to note that a double melting peak was formed by adding CSF particles. The explanation could be related to the formation of less perfect crystals that over the melting process can be melted, recrystallize into spherulites with thicker lamellar thicknesses and, therefore, re-melt at higher temperatures [64]. Kong et al. [65] also reported the double melting peak for the addition of eggshell in a PLA matrix. Nevertheless, the surface treatment of CSF

particles with GPS led to decrease the T_m up to 148.6 °C as well as slightly suppress the double melting peak. This fact is probably caused by the enhancement of interfacial adhesion that promotes the formation of crystalline structures with more perfect crystals than PLA/CSF composite. A similar result was reported by Luo et al. [66] with the addition of corn fibers treated with a combination of alkali and silane agent in a PLA matrix. In the case of composite with Xibond, ECO, and MCO compatibilizers, a single melting peak with similar T_m values was obtained. This indicates a homogenous crystalline structure with similar lamellar thicknesses. Related to enthalpies, the degree of crystallinity (X_c) of composites has been evaluated. Firstly, neat PLA presented an X_c value of 7.7%. According to the literature, the X_c of composites depends on the nucleation ability of each filler and its content [67]. In particular, the addition of CSF particles reduced the crystallinity to 1.2%, confirming that it interrupts the packing process of PLA chains, becoming a matrix almost amorphous. This effect was also in line with our previous studies using a different polymer matrix [19]. All compatibilized composites showed an evident increase of crystallinity compared to PLA/CSF composite, except for PLA/CSF_X that presents a slight increase. In the case of CSF particles treated with silane, the crystallinity was enhanced up to the value of 5.8% caused by the better interaction between phases that may increase the nucleation activity of manufactured composite [68]. Finally, for both ECO and MCO compatibilizers, its addition induced to increase the crystallinity to 5.1% and 7.5%, respectively, that is around 5 and 7 times higher regarding to PLA/CSF composite. The incorporation of functionalized vegetable oils resulted in a plasticization effect that increases the chain mobility and therefore favoring the crystal formation. Similar results were also reported by Quiles-Carillo et al. [56] with the addition of epoxidized soybean oil in PLA/orange peel flour composite. In this study, a X_c value of 8.31% was obtained compared to 5% of uncompatibilized composite, being a lower difference than present paper.

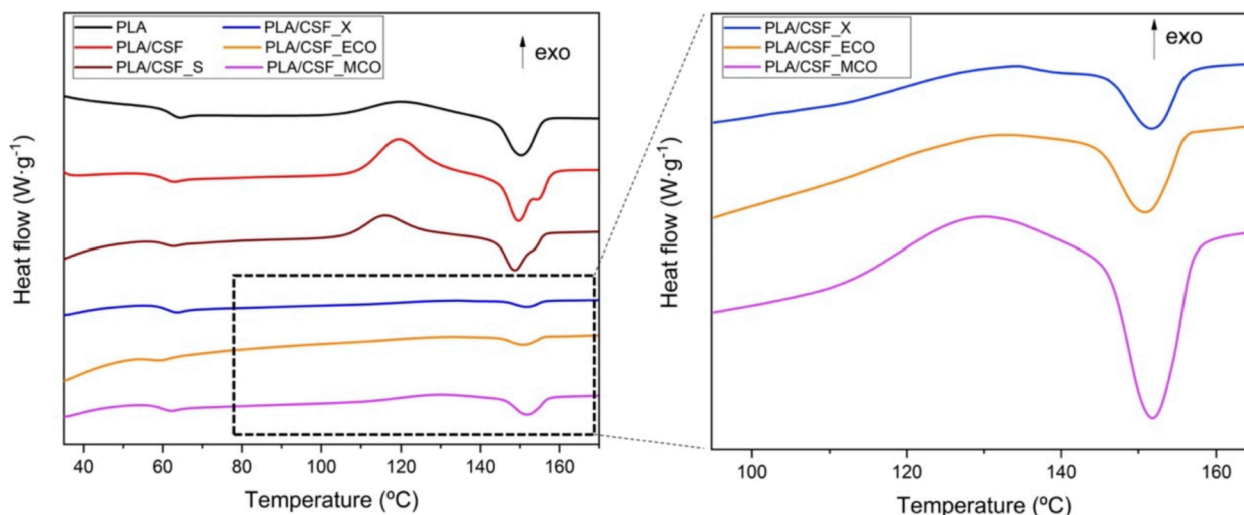The thermal degradation of neat PLA, CSF filler, and PLA/CSF

Fig. 6. Differential scanning calorimetry (DSC) of poly(lactic acid) (PLA) and 15 wt% chia seed flour (CSF) composites with different compatibilizers at 10 °C·min⁻¹.

composites with different compatibilizers is shown in Fig. 7. Firstly, the thermal degradation of CSF particles is characterized by four main weight losses steps: residual moisture removal, cellulose degradation, hemicellulose degradation, and, finally, lignin degradation. As shown in Fig. 7, the first step occurred in the 30–220 °C range, whereas at higher temperatures, from 220 °C to 700 °C, it was attributed to the thermal degradation of cellulose, hemicellulose, and lignin [69]. At the end of thermal degradation, the remaining weight loss can be attributed to the mineral content present in the filler. Similar behaviour was reported by Lee *et al.* [70] using bamboo fiber as a lignocellulosic filler.

Regarding composites manufactured, neat PLA was thermally degraded in a single step, as can be observed in Fig. 7(a). This drop was produced by chain-scission of macromolecules of PLA through the breakage of ester groups into smaller fragments [71]. The addition of CSF particles reduced the temperature required for 5 wt% of weight loss ($T_{5\%}$) from 328.4 °C for neat PLA up to 264.9 °C. As plotted in Fig. 7(a), PLA/CSF composite showed a reduction of the thermal stability associated with its low degradation temperature, which is characteristic of the presence of CSF fillers. Similar thermal degradation was reported by Qien and Sheng [62] with bamboo cellulose in PLA composites. Nevertheless, incorporating compatibilizers enhanced the thermal stability of manufactured composite, where $T_{5\%}$ is delayed approximately 45–50 °C for all compatibilizers compared to PLA/CSF composite. The significant difference when composites are compatibilized could be directly associated with the improvement of matrix-polymer interaction, which hinders the removal of volatile products over thermal degradation [37]. In addition, the maximum degradation rate temperature (T_{max}) was also determined by the first derivate of weight loss, as observed in Fig. 7(b). As expected, neat PLA presented the highest value of 390.9 °C, taking into account the absence of CSF fillers. On the contrary, the lowest T_{max} was observed for PLA/CSF composite with a value of 320.5 °C, being in concordance with the trend of $T_{5\%}$ value. As happened previously, the addition of compatibilizers also delayed the T_{max} values in the 353.8–359.9 °C range. It should point out that the highest improvement was obtained for PLA/CSF_ECO composite and this can be related to the higher reactivity with CSF filler and matrix compared to other compatibilizers. Furthermore, according to Agüero *et al.* [72], the epoxidized vegetable oils present low solubility in a PLA matrix, thus providing a thermal oxidation effect due to the non-reacted epoxy groups, whereas the remaining oil also could act as a physical barrier to hinder the volatile products.

3.5. Thermomechanical properties of PLA/CSF composites with compatibilizers

The evolution of storage modulus (G') and damping factor (tan δ) as a function of temperature for all manufactured composites are plotted in Fig. 8(a-b), respectively. Concerning storage modulus, neat PLA was characterized by a value of 1200 MPa at room temperature (30 °C), being the lowest G' value which is in concordance with the previous mechanical results. As expected, the addition of CSF filler increased the stiffness of composite up to 1600 MPa, which means an increment of 33.3% compared to neat PLA. This remarkable improvement in the mechanical resistance properties by the addition of lignocellulosic filler was also reported by several authors [73,74], explained by the mobility restriction of polymers chains. Nevertheless, the addition of compatibilizers caused a reduction of G' values regarding uncompatibilized PLA/CSF composite, thus indicating an increase of mechanical ductile properties. Aguero *et al.* [75] suggested that using a compatibilizer improves the compatibility between PLA and fillers and, therefore, increases the ductility. It should be remarked that the functionalized vegetable oils, i.e., ECO and MCO, provided the lowest G' value in the 1371–1400 MPa range, which corroborates the dual function of compatibilizer and plasticizer. At temperatures between 50 and 90 °C, the G' value sharply decreases due to the glass-rubber transition that corresponds to the T_g [76]. Over 90 °C, a second thermal transition was observed related to the rearrange of PLA chains into a more packed structure characterized by the cold crystallization process. During this process, both stiffness and density increase because of the highly ordered structure [77]. The incorporation of CSF in PLA matrix led to delay the cold crystallization process compared to neat PLA, indicating that CSF filler interrupts the packaging process of PLA matrix [21]. Regarding compatibilizers, in general, slight differences are shown compared to uncompatibilized composite under shear deformation stress as function of temperature, excepting for PLA/CSF_MCO. This shift to higher temperatures of PLA/CSF_MCO composite can be related to formation of macromolecular structures that delayed the cold crystallization as was described above [78]. After cold crystallization, the G' values obtained for all compatibilized composites were higher compared to neat PLA.

In relation to the damping factor (tan δ), it indicates the degree of molecular mobility and is used to estimate the T_g value. Neat PLA showed the lowest T_g value of 63 °C and was highly increased with the addition of CSF fillers up to 77 °C. This shift to higher temperatures suggests that CSF filler decreased the PLA molecular mobility, i.e., the
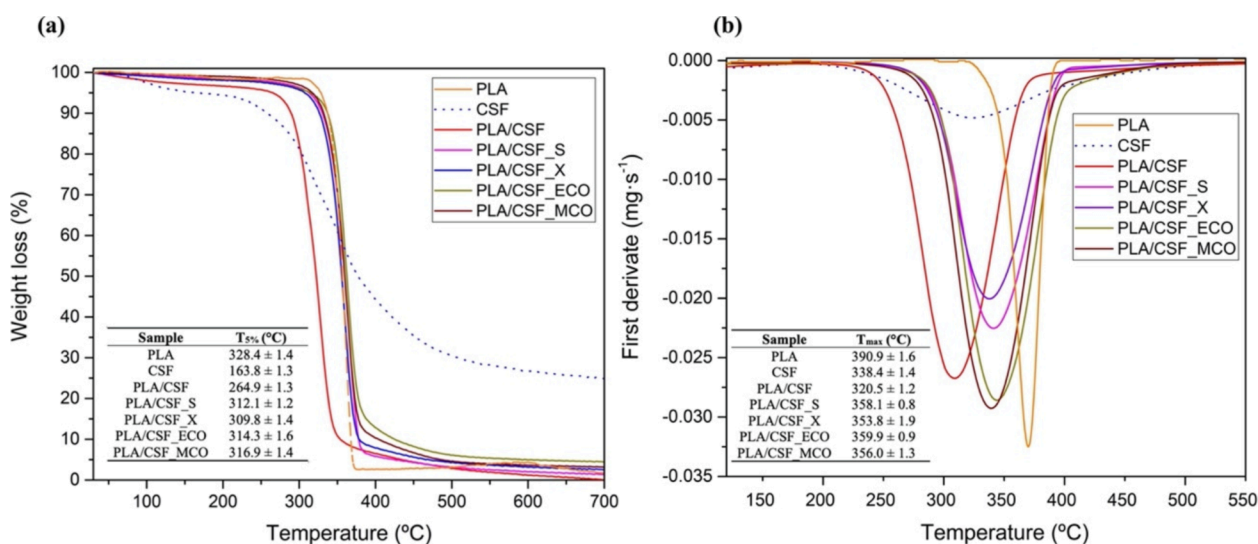

Fig. 7. (a) Thermogravimetric analysis (TGA) and (b) first derivate thermogravimetric (DTG) curves of poly(lactic acid) (PLA) and 15 wt% chia seed flour (CSF) composites with different compatibilizers.
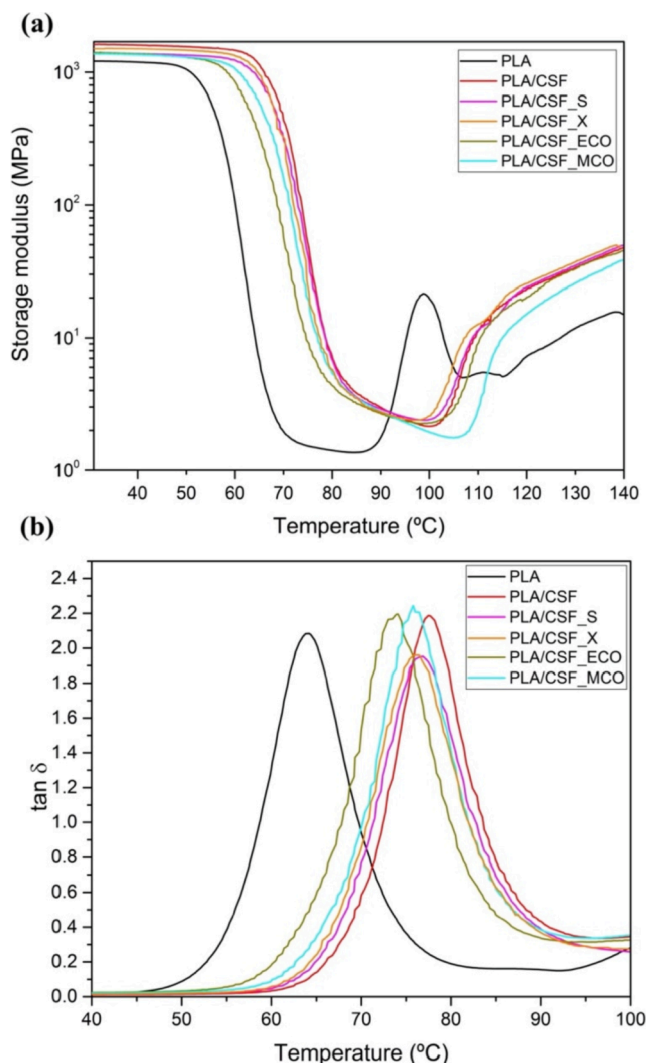
Fig. 8. Dynamic mechanical thermal analysis (DMTA) of poly(lactic acid) (PLA) and 15 wt% chia seed flour (CSF) composites with different compatibilizers; (a) storage modulus (G') and (b) damping factor (tan δ).

PLA chain was restricted. A similar remarkable increase was observed by other researchers with the addition of different lignocellulosic fillers in the PLA matrix [21]. With the addition of compatibilizers, a reduction of T_g value was observed, suggesting that manufactured composites presented higher chain mobility. In the case of PLA/CSF_S and PLA/CSF_X composites, it should be noted that the reduction of the T_g value was relatively low. Similar values were reported by Aguero *et al.* [25] that observed a slight decrease using Xibond and silane coupling agent as compatibilizers in PLA based on short flaxseed fibers. The addition of functionalized vegetable oils showed a much-pronounced T_g reduction. Both ECO and MCO compatibilizers enhanced the molecular chain mobility due to the flexibility provided by triglyceride molecules that lead to interact with CSF particles and PLA matrix. The PLA/CSF_ECO composite recorded a lower T_g value than using the MCO compatibilizer, indicating higher chain mobility as was above exposed in ductile and thermal properties. Then, the addition of both bio-based compatibilizers decreases the T_g by about 5–6% regarding PLA/CSF composite. This trend was also reported by Quiles-Carrillo *et al.* [79], who evaluated the effect of different compatibilizers such as aromatic carbodiimide, maleinized linseed oil, and epoxy-based styrene-acrylic monomer in PLA filled with almond shell flour (ASF).

3.6. Water uptake of PLA/CSF composites with compatibilizers

The evolution of water absorption of PLA/CSF composites with different compatibilizers after being submerged for 12 weeks is plotted in Fig. 9. Firstly, neat PLA presented the lowest water absorption with an approximately content of 0.75 wt%. This value corroborates the expected hydrophobic behaviour of PLA [80]. In agreement with the literature, the addition of lignocellulosic filler provides an increment of water absorption of the manufactured composite. The free hydroxyl groups (–OH) present in hemicellulose and cellulose may react with the hydrogen bonding of water [81]. In fact, the addition of CSF particles that present a hydrophilic nature led to increasing the water absorption of PLA/CSF composite up to 5.9 wt% after 12 weeks of immersion. Nevertheless, the addition of CSF with a previous silane treatment reduced the final water content up to 3 wt%, being a reduction of almost 50% compared to PLA/CSF composite. It is known that surface treatment of fillers with silanes reduced the availability of hydroxyl groups [82], and therefore, it decreased the water diffusion into the composite. The addition of copolymer Xibond also showed a reduction of water absorption compared to PLA/CSF composite. This result suggests that the available hydroxyl groups of CSF were reduced due to interaction with the copolymer, thus hindering the diffusion of water. Furthermore, the highest water absorption value recorded was 9.3 wt% for the MCO compatibilizer, meaning an increment of 57.6% regarding PLA/CSF composite. This behaviour can be attributed to the plasticization effect that increases the free volume and enhances the water diffusion into composite [13]. This trend is similar to one reported by Burgada *et al.* [83], who obtained the highest water absorption with a value of 7.5 wt% using maleinized linseed oil (MLO) in polypropylene with short hemp fiber. Comparing the PLA/CSF_MCO composite value with other studies, the water absorption is not considered high. Several studies have evaluated the water uptake by wood-plastic composites (WPCs) with values about 15–16% in HDPE-based WPCs [84] or even around 12% with PLA-based WPCs [85]. It is important to remark that a water uptake in WPCs of 25% is commonly accepted, being the minimum level to begin the decrease of mechanical properties and bacterial growth [86]. Therefore, water uptake of PLA/CSF_MCO composite can guarantee no growth of bacterial and dimensional stability to be used in outdoor applications. However, the addition of ECO recorded a value of 4.51 wt%, meaning a lower value than PLA/CSF and PLA/CSF_MCO composite. As shown, the addition of ECO and MCO provides different water absorption values despite both presenting the dual function of compatibilizer and
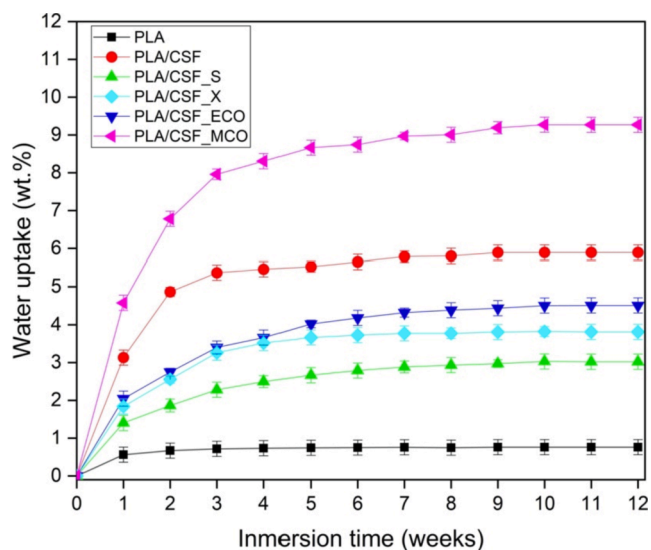

Fig. 9. Water uptake of poly(lactic acid) (PLA) and 15 wt% chia seed flour (CSF) composites with different compatibilizers.

plasticizer. This comparison of results suggests that PLA/CSF_ECO composite presents less available hydroxyl groups in CSF particles that can react further with water, thus reducing water absorption. As commented previously, the compatibilizing effect is related to interaction with lignocellulosic filler and PLA chains. Therefore, this phenomenon may be explained by a higher compatibilization effect, i.e., higher reactivity of ECO compared to MCO that reduces the water absorption of composite. This is in concordance with values obtained in TGA and DTG curves that show the highest thermal stability because of the high reactivity and, therefore, more interaction between CSF and PLA matrix. A similar finding was reported by Shafiq *et al.* [87] when the addition of epoxidized vegetable oil in polypropylene with rubber seed shell showed a decrease in water absorption compared to uncompatibilized composite.

3.7. Disintegration under composting conditions of PLA/CSF composites with compatibilizers

The weight loss of PLA/CSF composites with different compatibilizers was carried out to evaluate their effect on the disintegration process under composting conditions. The weight loss and the visual appearance can be observed in Figs. 10 and 11, respectively. At the beginning, i.e., zero-time, neat PLA presented its typical translucid appearance that becomes dark brown for the addition of CSF filler. The addition of compatibilizers slightly changed the colour appearance compared to PLA/CSF composite, as plotted in Fig. 10. After 4 days, no sign of weight loss was recorded for all composites, while an evident change in visual appearance was observed. Neat PLA showed a shift from translucid to opaque due to the increment of chain mobility that induced the crystallization of the PLA matrix. This effect is attributed to the proximity of the test temperature, which is 58 °C, to the T_g value of the sample [88]. The same behaviour was obtained for all PLA/CSF composites, where it is suggested that the opacity of the PLA matrix induces the samples to become whiter. This phenomenon was also reported by Balart *et al.* [46], who assessed the disintegration compost of PLA with hazelnut shell flour. On the 8th day, neat PLA and PLA/CSF composite recorded a weight loss of 14% and 23%, respectively, noting a visual aspect more brittle for PLA/CSF composite. According to Da silva *et al.* [89], lignocellulosic fillers, which are mainly composed of cellulose, hemicellulose, and lignin, can be degraded by microorganism action. Nevertheless, it has been previously reported in the literature that neat PLA disintegrates faster than composites with lignocellulosic filler

[90,91] due to the biodegradation rate of the lignocellulosic fillers is slower than PLA matrix [92]. In this case, PLA/CSF composites showed a contrary behavior, at least in the early incubation days. It is known that the hydrophilic nature of lignocellulosic fillers leads to transfer water as well as enzymes or microorganism easily into the composite that induces to increase the degradation rate [68]. Moreover, the microorganism action is faster in amorphous domains [80,93], and therefore, PLA/CSF composite presented a higher weight loss than neat PLA due to its low crystallinity. For all PLA/CSF composites with compatibilizers, the disintegration rate was delayed, recording values lower than 2%. This reduction can be ascribed to better compatibility between CSF filler and PLA matrix as well as the effect of crystallinity and water uptake. On the 11th day, all compatibilized PLA/CSF composites, that presented a disintegration rate lower than PLA/CSF composite and neat PLA, started to lose a significantly higher value than 10% except for PLA/CSF_ECO composite. On the 15th day, a remarkable increase in weight loss was recorded, particularly for the PLA/CSF composite with a value of 80%. On the contrary, both epoxidized and maleinized vegetable oils showed the lowest weight loss, being 10% and 30%, respectively. It should be pointed out that although PLA/CSF_ECO composite presented less crystallinity than PLA/CSF_MCO composite, the water uptake was highly reduced which hinders the disintegration rate. This difference was also corroborated with no breakage in visual appearance. After 18th day, neat PLA showed the highest degradation rate, about 88%, which was above of PLA/CSF composite. After 31 days, neat PLA was totally disintegrated as expected due to its biodegradability, while all PLA/CSF composites presented a similar weight loss in the 94–90% range although the initial degradation rate was different. These results suggest that, irrespective of the compatibilizer used, after 31 days of testing, the rate of disintegration by composting is the same. Therefore, it can be concluded that all bio-based novel manufactured composites are considered disintegrable regardless the compatibilizer employed.

4. Conclusion

Novel green composites based on PLA and CSF filler at 15 wt% have been developed. The poor interfacial adhesion between CSF filler and PLA was improved by testing four different compatibilizers. FTIR results suggested chemical interaction in all compatibilized composites. The mechanical properties showed different results depending on the compatibilizer employed. Both PLA/CSF_S and PLA/CSF_X composite obtained an increment of mechanical resistance, toughness, and hardness. In the case of modified chia seed oil by epoxidation and maleinization, the ductile properties were remarkably improved, attaining the highest elongation at break, which means 10 and 8 times higher regarding the PLA/CSF composite, respectively. The enhancement of interfacial adhesion between CSF fillers and PLA matrix was also corroborated by the surface morphology of the fractured surfaces, where this enhancement was observed. Thermal properties of all compatibilized composites pointed to a higher crystallinity than PLA/CSF composite, suggesting an improvement of chain mobility. Furthermore, the addition of compatibilizers caused a delay of 33–39 °C in the maximum degradation rate confirming the higher polymer-matrix interaction, highlighting PLA/CSF_ECO composite with a value of 360 °C. Concerning DMTA analysis, Tg values were reduced compared to PLA/CSF composite indicating higher chain mobility provided by the addition of compatibilizers, particularly for PLA/CSF_ECO composite. In general, the water uptake was reduced using compatibilizers due to the decrease of available hydroxyl groups that can react with water further. In particular, PLA/CSF_MCO presented the highest value, which is 100% higher than PLA/CSF_ECO, because of its lower reactivity that induces water diffusion into the composite. Finally, the disintegration test concluded that the use of different compatibilizers did not affect the compostability of composites, being an advantage considering all properties provided. Therefore, as a general conclusion, it has been developed composites based on PLA and by-products coming from CO extraction industry. The
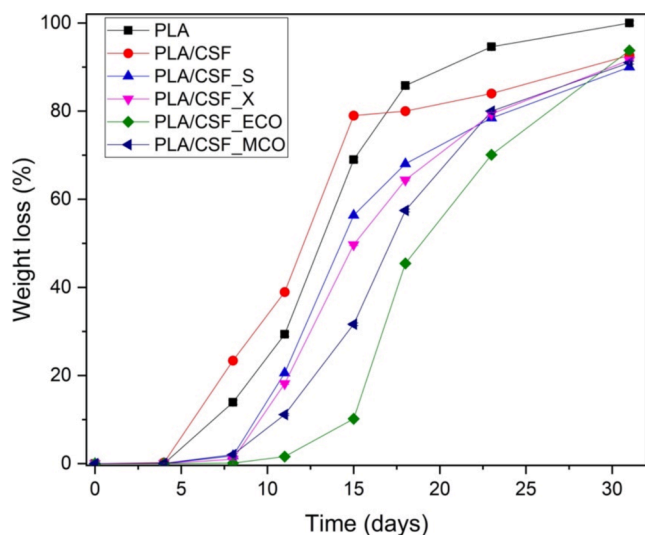

Fig. 10. Weight loss during the disintegration process in controlled compost oil of poly(lactic acid) (PLA) and 15 wt% chia seed flour (CSF) composites with different compatibilizers.

Fig. 11. Visual appearance of the disintegration process in controlled compost oil of poly(lactic acid) (PLA) and 15 wt% chia seed flour (CSF) composites with different compatibilizers.
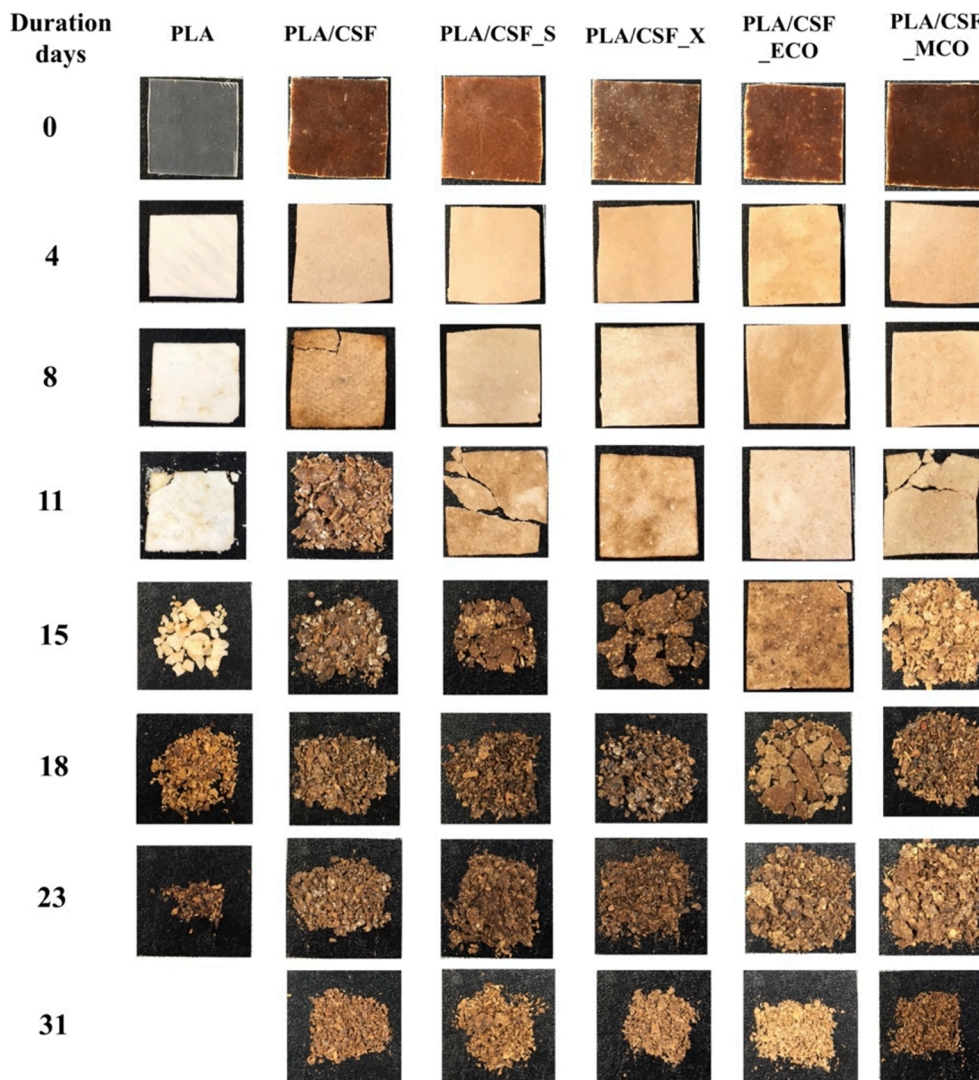
addition of CSF in PLA matrix gives high added value to the waste contributing to the circular economy. Besides, the novel bio-based compatibilizers and plasticizers derived from chia seed oil such as ECO and MCO, were employed for the first time with the aim of improving the polymer-matrix interaction. The results shows that PLA with CSF by using the novel compatibilizers from the same seed, are an interesting proposal from both economic and environmental point of view to be applied at industrial level to manufacture fully renewable composites.

CRediT authorship contribution statement

Ivan Dominguez-Candela: Conceptualization, Validation, Investigation, Writing – original draft. **Jaume Gomez-Caturla:** Validation, Formal analysis, Software. **S.C. Cardona:** Resources, Writing – review & editing. **Jaime Lora-García:** Resources, Visualization, Supervision. **Vicent Fombuena:** Conceptualization, Resources, Writing – review & editing, Supervision, Project administration.

Declaration of Competing Interest

The authors declare that they have no known competing financial interests or personal relationships that could have appeared to influence the work reported in this paper.

References

[1] P. Europe, Plastics–the facts 2020: An Analysis of European Plastics Production, Demand and Waste. Plastics Europe, Brussels. Available online: https://plasticseurope.org/wp-content/uploads/2021/09/Plastics_the_facts-WEB-2020_versionJun21_final.pdf (accessed on 21 September 2021).
[2] K. Leja, G. Lewandowicz, Polymer biodegradation and biodegradable polymers-a review, Polish J. Environ. Stud. 19 (2010).
[3] Data BM. European Bioplastics. Available online: wwweuropean-bioplasticsorg/market (accessed on 20 October 2021), 2017.
[4] S. Kocaman, M. Karaman, M. Gursoy, G. Ahmetli, Chemical and plasma surface modification of lignocellulose coconut waste for the preparation of advanced biobased composite materials, Carbohydr. Polym. 159 (2017) 48–57.

[5] S. Torres-Giner, N. Montanes, O. Fenollar, D. García-Sanoguera, R. Balart, Development and optimization of renewable vinyl plastisol/wood flour composites exposed to ultraviolet radiation, Mater. Des. 108 (2016) 648–658.

[6] W. Zhang, X. Zhang, M. Liang, C. Lu, Mechanochemical preparation of surface-acetylated cellulose powder to enhance mechanical properties of cellulose-filler-reinforced NR vulcanizates, Compos. Sci. Technol. 68 (12) (2008) 2479–2484.

[7] X. Yan, M. Diao, Y. Yu, F. Gao, E. Wang, Z. Wang, T. Zhang, Influence of esterification and ultrasound treatment on formation and properties of starch nanoparticles and their impact as a filler on chitosan based films characteristics, Int. J. Biol. Macromol. 179 (2021) 154–160.

[8] S. Ikhlef, S. Nekkaa, M. Guessoum, N. Haddaoui, Effects of alkaline treatment on the mechanical and rheological properties of low-density polyethylene/spartium junceum flour composites, International Scholarly Research Notices. 2012 (2012) 1–7.

[9] N.A. Maziad, D.E. EL-Nashar, E.M. Sadek, The effects of a silane coupling agent on properties of rice husk-filled maleic acid anhydride compatibilized natural rubber/low-density polyethylene blend, J. Mater. Sci. 44 (10) (2009) 2665–2673.

[10] L.A. Pothan, S. Thomas, Polarity parameters and dynamic mechanical behaviour of chemically modified banana fiber reinforced polyester composites, Compos. Sci. Technol. 63 (9) (2003) 1231–1240.

[11] Y. Xie, C.A.S. Hill, Z. Xiao, H. Militz, C. Mai, Silane coupling agents used for natural fiber/polymer composites: A review, Compos. A Appl. Sci. Manuf. 41 (7) (2010) 806–819.

[12] C. Nyambo, A.K. Mohanty, M. Misra, Effect of maleated compatibilizer on performance of PLA/wheat Straw-Based green composites, Macromol. Mater. Eng. 296 (8) (2011) 710–718.

[13] J. Ferri, D. Garcia-Garcia, L. Sánchez-Nacher, O. Fenollar, R. Balart, The effect of maleinized linseed oil (MLO) on mechanical performance of poly (lactic acid)-thermoplastic starch (PLA-TPS) blends, Carbohydr. Polym. 147 (2016) 60–68.

[14] M.J. Garcia-Campo, L. Quiles-Carrillo, J. Masia, M.J. Reig-Pérez, N. Montanes, R. Balart, Environmentally friendly compatibilizers from soybean oil for ternary blends of poly (lactic acid)-PLA, poly (ε-caprolactone)-PCL and poly (3-hydroxybutyrate)-PHB, Materials. 10 (2017) 1339.

[15] A. Retegi, I. Algar, L. Martin, F. Altuna, P. Stefani, R. Zuluaga, P. Gañán, I. Mondragon, Sustainable optically transparent composites based on epoxidized soy-bean oil (ESO) matrix and high contents of bacterial cellulose (BC), Cellulose 19 (1) (2012) 103–109.

[16] M. Samper, R. Petrucci, L. Sánchez-Nacher, R. Balart, J. Kenny, New environmentally friendly composite laminates with epoxidized linseed oil (ELO) and slate fiber fabrics, Compos. B Eng. 71 (2015) 203–209.

[17] I. Dominguez-Candela, J.M. Ferri, S.C. Cardona, J. Lora, V. Fombuena, Dual Plasticizer/Thermal Stabilizer Effect of Epoxidized Chia Seed Oil (Salvia hispanica L.) to Improve Ductility and Thermal Properties of Poly (Lactic Acid), Polymers. 13 (8) (2021;13:1283.) 1283.

[18] Chia Seeds Market Size Worth $4.7 Billion By 2025. Grand View Research. 2019. Available online: https://www.grandviewresearch.com/press-release/global-chia-seeds-market (accessed on 14 October 2021).

[19] I. Dominguez-Candela, D. Garcia-Garcia, A. Perez-Nakai, J. Lora, V. Fombuena, Contribution to a Circular Economy Model: From Lignocellulosic Wastes from the Extraction of Vegetable Oils to the Development of a New Composite, Polymers. 13 (2021) 2269.

[20] A. Lerma-Canto, J. Gomez-Caturla, M. Herrero-Herrero, D. Garcia-Garcia, V. Fombuena, Development of Polylactic Acid Thermoplastic Starch Formulations Using Maleinized Hemp Oil as Biobased Plasticizer, Polymers. 13 (2021) 1392.

[21] A. Carbonell-Verdu, T. Boronat, L. Quiles-Carrillo, O. Fenollar, F. Dominici, L. Torre, Valorization of Cotton Industry Byproducts in Green Composites with Polylactide, J. Polym. Environ. 28 (7) (2020) 2039–2053.

[22] T.P.T. Tran, J.-C. Bénézet, A. Bergeret, Rice and Einkorn wheat husks reinforced poly (lactic acid)(PLA) biocomposites: Effects of alkaline and silane surface treatments of husks, Ind. Crops Prod. 58 (2014) 111–124.

[23] L. Quiles-Carrillo, T. Boronat, N. Montanes, R. Balart, S. Torres-Giner, Injection-molded parts of fully bio-based polyamide 1010 strengthened with waste derived slate fibers pretreated with glycidyl-and amino-silane coupling agents, Polym. Test. 77 (2019) 105875.

[24] M.D. Samper, R. Petrucci, L. Sánchez-Nacher, R. Balart, J.M. Kenny, Effect of silane coupling agents on basalt fiber–epoxidized vegetable oil matrix composite materials analyzed by the single fiber fragmentation technique, Polym. Compos. 36 (7) (2015) 1205–1212.

[25] Á. Agüero, D. Garcia-Sanoguera, D. Lascano, S. Rojas-Lema, J. Ivorra-Martinez, O. Fenollar, S. Torres-Giner, Evaluation of different compatibilization strategies to improve the performance of injection-molded green composite pieces made of polylactide reinforced with short flaxseed fibers, Polymers. 12 (4) (2020) 821.

[26] M.P. Arrieta, M.D. Samper, J. López, A. Jiménez, Combined effect of poly (hydroxybutyrate) and plasticizers on polylactic acid properties for film intended for food packaging, J. Polym. Environ. 22 (4) (2014) 460–470.

[27] M.S. San Román, M.J. Holgado, B. Salinas, V. Rives, Drug release from layered double hydroxides and from their polylactic acid (PLA) nanocomposites, Appl. Clay Sci. 71 (2013) 1–7.

[28] B. Braun, J.R. Dorgan, S.F. Dec, Infrared spectroscopic determination of lactide concentration in polylactide: an improved methodology, Macromolecules 39 (2006) 9302–9310.

[29] T. Kemala, E. Budianto, B. Soegiyono, Preparation and characterization of microspheres based on blend of poly (lactic acid) and poly (ε-caprolactone) with poly (vinyl alcohol) as emulsifier, Arabian J. Chem. 5 (1) (2012) 103–108.

[30] S. Torres-Giner, J.V. Gimeno-Alcañiz, M.J. Ocio, J.M. Lagaron, Optimization of electrospun polylactide-based ultrathin fibers for osteoconductive bone scaffolds, J. Appl. Polym. Sci. 122 (2) (2011) 914–925.

[31] E.M.B. Lima, A. Middea, R. Neumann, R.M.d.S.M. Thiré, J.F. Pereira, S.C. Freitas, M.S. Penteado, A.M. Lima, A.P.d.S. Minguita, M.d.C. Mattos, A.d.S. Teixeira, I.C. S. Pereira, N.R. Rojas dos Santos, J.M. Marconcini, R.N. Oliveira, A.C. Corrêa, Biocomposites of PLA and Mango Seed Waste: Potential Material for Food Packaging and a Technological Alternative to Reduce Environmental Impact, Starch-Stärke. 73 (5-6) (2021) 2000118.

[32] E.M.B. Lima, A.M. Lima, A.P.S. Minguita, N.R. Rojas dos Santos, I.C.S. Pereira, T.T. M. Neves, L.F. da Costa Gonçalves, A.P.D. Moreira, A. Middea, R. Neumann, M.I. B. Tavares, R.N. Oliveira, Poly (lactic acid) biocomposites with mango waste and organo-montmorillonite for packaging, J. Appl. Polym. Sci. 136 (21) (2019) 47512.

[33] L. Wan, Y. Zhang, Jointly modified mechanical properties and accelerated hydrolytic degradation of PLA by interface reinforcement of PLA-WF, J. Mech. Behav. Biomed. Mater. 88 (2018) 223–230.

[34] R. Sepe, F. Bollino, L. Boccarusso, F. Caputo, Influence of chemical treatments on mechanical properties of hemp fiber reinforced composites, Compos. B Eng. 133 (2018) 210–217.

[35] T. Yu, J. Ren, S. Li, H. Yuan, Y. Li, Effect of fiber surface-treatments on the properties of poly (lactic acid)/ramie composites, Compos. Part A: Appl. Sci. Manuf., 41 (2010) 499-505.

[36] D. García-García, A. Carbonell, M. Samper, D. García-Sanoguera, R. Balart, Green composites based on polypropylene matrix and hydrophobized spend coffee ground (SCG) powder, Compos. B Eng. 78 (2015) 256–265.

[37] L. Quiles-Carrillo, R. Balart, T. Boronat, S. Torres-Giner, D. Puglia, F. Dominici, L. Torre, Development of Compatibilized Polyamide 1010/Coconut Fibers Composites by Reactive Extrusion with Modified Linseed Oil and Multi-functional Petroleum Derived Compatibilizers, Fibers Polym. 22 (3) (2021) 728–744.

[38] A. Masek, S. Cichosz, M. Piotrowska, Biocomposites of Epoxidized Natural Rubber/Poly (lactic acid) Modified with Natural Fillers (Part I), Int. J. Mol. Sci. 22 (2021) 3150.

[39] F. Pawlak, M. Aldas, J. López-Martínez, M.D. Samper, Effect of different compatibilizers on injection-molded green fiber-reinforced polymers based on poly (lactic acid)-maleinized linseed oil system and sheep wool, Polymers. 11 (2019) 1514.

[40] Chen T, Wu Y, Qiu J, Fei M, Qiu R, Liu W. Interfacial compatibilization via in-situ polymerization of epoxidized soybean oil for bamboo fibers reinforced poly (lactic acid) biocomposites. Composites Part A: Applied Science and Manufacturing. 2020; 138:106066.

[41] Kamarudin SH, Abdullah LC, Aung MM, Ratnam CT, Jusoh ER. A study of mechanical and morphological properties of PLA based biocomposites prepared with EJO vegetable oil based plasticiser and kenaf fibres. Materials Research Express. 2018;5:085314.

[42] S. Mahmud, Y.u. Long, J. Wang, J. Dai, R. Zhang, J. Zhu, Waste cellulose fibers reinforced polylactide toughened by direct blending of epoxidized soybean oil, Fibers Polym. 21 (12) (2020) 2949–2961.

[43] A.N. Frone, S. Berlioz, J.-F. Chailan, D.M. Panaitescu, D. Donescu, Cellulose fiber-reinforced polylactic acid, Polym. Compos. 32 (6) (2011) 976–985.

[44] K. Madhavan Nampoothiri, N.R. Nair, R.P. John, An overview of the recent developments in polylactide (PLA) research, Bioresour. Technol. 101 (22) (2010) 8493–8501.

[45] S. Angelini, P. Cerruti, B. Immirzi, G. Santagata, G. Scarinzi, M. Malinconico, From biowaste to bioresource: Effect of a lignocellulosic filler on the properties of poly (3-hydroxybutyrate), Int. J. Biol. Macromol. 71 (2014) 163–173.

[46] J. Balart, V. Fombuena, O. Fenollar, T. Boronat, L. Sánchez-Nacher, Processing and characterization of high environmental efficiency composites based on PLA and hazelnut shell flour (HSF) with biobased plasticizers derived from epoxidized linseed oil (ELO), Compos. B Eng. 86 (2016) 168–177.

[47] S.H. Kamarudin, L.C. Abdullah, M.M. Aung, C.T. Ratnam, Mechanical and physical properties of Kenaf-reinforced Poly (lactic acid) plasticized with epoxidized Jatropha Oil, BioResources. 14 (2019) 9001–9020.

[48] B.W. Chieng, N.A. Ibrahim, Y.Y. Then, Y.Y. Loo, Epoxidized vegetable oils plasticized poly (lactic acid) biocomposites: mechanical, thermal and morphology properties, Molecules 19 (2014) 16024–16038.

[49] S. Mahmud, Y.u. Long, M. Abu Taher, Z. Xiong, R. Zhang, J. Zhu, Toughening polylactide by direct blending of cellulose nanocrystals and epoxidized soybean oil, J. Appl. Polym. Sci. 136 (46) (2019) 48221.

[50] P. Liminana, D. Garcia-Sanoguera, L. Quiles-Carrillo, R. Balart, N. Montanes, Development and characterization of environmentally friendly composites from poly (butylene succinate)(PBS) and almond shell flour with different compatibilizers, Compos. B Eng. 144 (2018) 153–162.

[51] D. Lascano, D. Garcia-Garcia, S. Rojas-Lema, L. Quiles-Carrillo, R. Balart, T. Boronat, Manufacturing and characterization of green composites with partially biobased epoxy resin and flaxseed flour wastes, Applied Sciences. 10 (2020) 3688.

[52] J.E. Crespo, R. Balart, L. Sanchez, J. Lopez, Mechanical behaviour of vinyl plastisols with cellulosic fillers. Analysis of the interface between particles and matrices, Int. J. Adhes. Adhes. 27 (5) (2007) 422–428.

[53] K.S. Chun, S. Husseinsyah, H. Osman, Mechanical and thermal properties of coconut shell powder filled polylactic acid biocomposites: effects of the filler content and silane coupling agent, J. Polym. Res. 19 (2012) 1–8.

[54] N. Moazeni, Z. Mohamad, N. Dehbari, Study of silane treatment on poly-lactic acid (PLA)/sepiolite nanocomposite thin films, J. Appl. Polym. Sci. 132 (6) (2015) n/a–n/a.

[55] A. Carbonell-Verdu, M.D. Samper, D. Garcia-Garcia, L. Sanchez-Nacher, R. Balart, Plasticization effect of epoxidized cottonseed oil (ECSO) on poly (lactic acid), Ind. Crops Prod. 104 (2017) 278–286.

[56] L. Quiles-Carrillo, N. Montanes, J.M. Lagaron, R. Balart, S. Torres-Giner, On the use of acrylated epoxidized soybean oil as a reactive compatibilizer in injection-molded compostable pieces consisting of polylactide filled with orange peel flour, Polym. Int. 67 (10) (2018) 1341–1351.

[57] L. Gonzalez, A. Agüero, L. Quiles-Carrillo, D. Lascano, N. Montanes, Optimization of the loading of an environmentally friendly compatibilizer derived from linseed oil in poly (lactic acid)/diatomaceous earth composites, Materials. 12 (2019) 1627.

[58] P.J. Jandas, S. Mohanty, S.K. Nayak, Thermal properties and cold crystallization kinetics of surface-treated banana fiber (BF)-reinforced poly (lactic acid)(PLA) nanocomposites, J. Therm. Anal. Calorim. 114 (3) (2013) 1265–1278.

[59] D.L. Ortiz-Barajas, J.A. Arévalo-Prada, O. Fenollar, Y.J. Rueda-Ordóñez, S. Torres-Giner, Torrefaction of Coffee Husk Flour for the Development of Injection-Molded Green Composite Pieces of Polylactide with High Sustainability, Applied Sciences. 10 (2020) 6468.

[60] A. Gregorova, M. Hrabalova, R. Kovalcik, R. Wimmer, Surface modification of spruce wood flour and effects on the dynamic fragility of PLA/wood composites, Polym. Eng. Sci. 51 (1) (2011) 143–150.

[61] M.L. Sanyang, S.M. Sapuan, M. Jawaid, M.R. Ishak, J. Sahari, Effect of plasticizer type and concentration on tensile, thermal and barrier properties of biodegradable films based on sugar palm (Arenga pinnata) starch, Polymers. 7 (2015) 1106–1124.

[62] S. Qian, K. Sheng, PLA toughened by bamboo cellulose nanowhiskers: Role of silane compatibilization on the PLA bionanocomposite properties, Compos. Sci. Technol. 148 (2017) 59–69.

[63] Y.-M. Corre, J. Duchet, J. Reignier, A. Maazouz, Melt strengthening of poly (lactic acid) through reactive extrusion with epoxy-functionalized chains, Rheol. Acta 50 (7-8) (2011) 613–629.

[64] A. Orue, A. Eceiza, A. Arbelaiz, Preparation and characterization of poly (lactic acid) plasticized with vegetable oils and reinforced with sisal fibers, Ind. Crops Prod. 112 (2018) 170–180.

[65] J. Kong, C. Han, Y. Yu, L. Dong, Production and characterization of sustainable poly (lactic acid)/functionalized-eggshell composites plasticized by epoxidized soybean oil, J. Mater. Sci. 53 (20) (2018) 14386–14397.

[66] H. Luo, C. Zhang, G. Xiong, Y. Wan, Effects of alkali and alkali/silane treatments of corn fibers on mechanical and thermal properties of its composites with polylactic acid, Polym. Compos. 37 (12) (2016) 3499–3507.

[67] L. Ludueña, A. Vázquez, V. Alvarez, Effect of lignocellulosic filler type and content on the behavior of polycaprolactone based eco-composites for packaging applications, Carbohydr. Polym. 87 (1) (2012) 411–421.

[68] B. Calabia, F. Ninomiya, H. Yagi, A. Oishi, K. Taguchi, M. Kunioka, M. Funabashi, Biodegradable poly (butylene succinate) composites reinforced by cotton fiber with silane coupling agent, Polymers. 5 (1) (2013) 128–141.

[69] V. Tserki, P. Matzinos, S. Kokkou, C. Panayiotou, Novel biodegradable composites based on treated lignocellulosic waste flour as filler. Part I. Surface chemical modification and characterization of waste flour, Compos. A Appl. Sci. Manuf. 36 (7) (2005) 965–974.

[70] S.-H. Lee, S. Wang, Biodegradable polymers/bamboo fiber biocomposite with bio-based coupling agent, Compos. A Appl. Sci. Manuf. 37 (1) (2006) 80–91.

[71] P.E. Sánchez-Jiménez, L.A. Pérez-Maqueda, A. Perejón, J.M. Criado, Generalized kinetic master plots for the thermal degradation of polymers following a random scission mechanism, The Journal of Physical Chemistry A. 114 (30) (2010) 7868–7876.

[72] Á. Agüero, D. Lascano, D. Garcia-Sanoguera, O. Fenollar, S. Torres-Giner, Valorization of linen processing by-products for the development of injection-molded green composite pieces of polylactide with improved performance, Sustainability. 12 (2020) 652.

[73] E. Părpăriţă, R.N. Darie, C.-M. Popescu, M.A. Uddin, C. Vasile, Structure–morphology–mechanical properties relationship of some polypropylene/lignocellulosic composites, Mater. Des. 56 (2014) 763–772.

[74] S. Agustin-Salazar, P. Cerruti, L.Á. Medina-Juárez, G. Scarinzi, M. Malinconico, H. Soto-Valdez, N. Gamez-Meza, Lignin and holocellulose from pecan nutshell as reinforcing fillers in poly (lactic acid) biocomposites, Int. J. Biol. Macromol. 115 (2018) 727–736.

[75] A. Aguero, L. Quiles-Carrillo, A. Jorda-Vilaplana, O. Fenollar, N. Montanes, Effect of different compatibilizers on environmentally friendly composites from poly (lactic acid) and diatomaceous earth, Polym. Int. 68 (5) (2019) 893–903.

[76] R. Al-Itry, K. Lamnawar, A. Maazouz, N. Billon, C. Combeaud, Effect of the simultaneous biaxial stretching on the structural and mechanical properties of PLA, PBAT and their blends at rubbery state, Eur. Polym. J. 68 (2015) 288–301.

[77] Y. Yu, Y. Cheng, J. Ren, E. Cao, X. Fu, W. Guo, Plasticizing effect of poly (ethylene glycol) s with different molecular weights in poly (lactic acid)/starch blends, J. Appl. Polym. Sci. 132 (16) (2015) n/a–n/a.

[78] V. Ojijo, S.S. Ray, Super toughened biodegradable polylactide blends with non-linear copolymer interfacial architecture obtained via facile in-situ reactive compatibilization, Polymer 80 (2015) 1–17.

[79] L. Quiles-Carrillo, N. Montanes, D. Garcia-Garcia, A. Carbonell-Verdu, R. Balart, S. Torres-Giner, Effect of different compatibilizers on injection-molded green composite pieces based on polylactide filled with almond shell flour, Compos. B Eng. 147 (2018) 76–85.

[80] M. Deroiné, A. Le Duigou, Y.-M. Corre, P.-Y. Le Gac, P. Davies, G. César, et al. Accelerated ageing of polylactide in aqueous environments: Comparative study between distilled water and seawater, Polym. Degrad. Stabil., 108 (2014) 319-329.

[81] S. Kuciel, P. Jakubowska, P. Kuźniar, A study on the mechanical properties and the influence of water uptake and temperature on biocomposites based on polyethylene from renewable sources, Compos. B Eng. 64 (2014) 72–77.

[82] J. Gironès, J.A. Méndez, S. Boufi, F. Vilaseca, P. Mutjé, Effect of silane coupling agents on the properties of pine fibers/polypropylene composites, J. Appl. Polym. Sci. 103 (6) (2007) 3706–3717.

[83] F. Burgada, E. Fages, L. Quiles-Carrillo, D. Lascano, J. Ivorra-Martinez, M. P. Arrieta, O. Fenollar, Upgrading Recycled Polypropylene from Textile Wastes in Wood Plastic Composites with Short Hemp Fiber, Polymers. 13 (8) (2021) 1248.

[84] M.H. Ab Ghani, S. Ahmad, The comparison of water absorption analysis between counterrotating and corotating twin-screw extruders with different antioxidants content in wood plastic composites, Adv. Mater. Sci. Eng. 2011 (2011) 1–4.

[85] R. Liu, Y. Peng, J. Cao, Y. Chen, Comparison on properties of lignocellulosic flour/polymer composites by using wood, cellulose, and lignin flours as fillers, Compos. Sci. Technol. 103 (2014) 1–7.

[86] R.A. Zabel, J.J. Morrell, Wood microbiology: decay and its prevention, Academic press, 2012.

[87] M.D. Shafiq, IsH. The effect of epoxidized vegetable oil and phthalic anhydride as compatibilizers on properties of rubber seed shell/polypropylene composites. Iranian Polymer Journal. 2021;30:547-57.

[88] D. Garcia-Garcia, A. Carbonell-Verdu, M. Arrieta, J. López-Martínez, M. Samper, Improvement of PLA film ductility by plasticization with epoxidized karanja oil, Polym. Degrad. Stabil. 179 (2020) 109259.

[89] A.M.B. da Silva, A.B. Martins, R.M.C. Santana, Biodegradability studies of lignocellulosic fiber reinforced composites, Elsevier, Fiber Reinforced Composites, 2021, pp. 241–271.

[90] A.P. Mathew, K. Oksman, M. Sain, Mechanical properties of biodegradable composites from poly lactic acid (PLA) and microcrystalline cellulose (MCC), J. Appl. Polym. Sci. 97 (5) (2005) 2014–2025.

[91] R. Kumar, M.K. Yakubu, R.D. Anandjiwala, Biodegradation of flax fiber reinforced poly lactic acid. eXPRESS, Polymer Letters. 4 (7) (2010) 423–430.

[92] As'ad Zandi, A. Zanganeh, F. Hemmati, J. Mohammadi-Roshandeh, Thermal and biodegradation properties of poly (lactic acid)/rice straw composites: effects of modified pulping products, Iran. Polym. J. 28 (5) (2019) 403–415.

[93] Y.-B. Luo, X.-L. Wang, Y.-Z. Wang, Effect of TiO2 nanoparticles on the long-term hydrolytic degradation behavior of PLA, Polym. Degrad. Stab. 97 (5) (2012) 721–728.